Supersonic Moist Air Flow with Condensation in a Wavy Wall Channel

Soon-Bum Kwon
Professor, School of Mechanical Engineering, Kyungpook National University
Hyung-Joon Ahn*†
Principal Researcher, Regulatory Research Division, Korea Institute of Nuclear Safety

The characteristics of Prandtl-Meyer expansion of supersonic flow with condensation along a wavy wall in a channel are investigated by means of experiments and numerical analyses. Experiments are carried out for the case of moist air flow in an intermittent indraft supersonic wind tunnel. The flow fields are visualized by a Schlieren system and the distributions of static pressure along the upper wavy wall are measured by a scanning valve system with pressure transducers. In numerical analyses, the distributions of streamlines, Mach lines, iso-pressure lines, and iso-mass fractions of liquid are obtained by the two-dimensional direct marching method of characteristics. The effects of stagnation temperature, absolute humidity, and attack angle of the upper wavy wall on the generation and the locations of generation and reflection of an oblique shock wave are clarified. Futhermore, it is confirmed that the wavy wall plays an important role in the generation of an oblique shock wave and that the effect of condensation on the flow fields is apparent.

Key Words : Supersonic Flow, Condensation Shock Wave, Oblique Shock Wave, Wavy Wall, Method of Characteristics, Moist Air

Nomenclature

A : Amplitude of wavy wall (mm)
L : Period of wavy wall (mm)
M : Mach number
p : Pressure (kPa)
T : Temperature (K)
ϕ : Relative humidity (%)
θ : Attack angle (degree)
w : Absolute humidity

Subscripts

0 : Stagnation point
e : Entrance of wavy wall
ω : Wall

† First Author
* Corresponding Author,
E-mail : k096ahj@kins.re.kr
TEL : +82-42-868-0156; **FAX** : +82-42-861-9945
19 Kusong-dong, Yousong-ku, Taejon 305-338, Korea.
(Manuscript **Received** August 16, 2000; **Revised** January 29, 2001)

1. Introduction

The acceleration of compressible vapor to a high speed results in a change of state which, depending on the amount of expansion and the closeness of the original state to the saturation condition, may change the vapor from an unsaturated state to a supersaturated state. At this state, the supersaturated vapor condenses with a nonequilibrium process of coalescence of vapor molecules. If condensation occurs, small liquid droplets can be observed along with consequent changes in the properties of flowing vapor, which are due primarily to the release of latent heat by the vapor as it condenses.

When an object like an airfoil is flown supersonically in a condensable gas such as moist air or water vapor, expansion and compression waves, oblique shock and condensation shock waves with a nonequilibrium process of conden-

sation may occur.

This kind of supersonic flow becomes very complicated, while similar flows may arise often in many industrial fields, such as the flow through a supersonic flight projectile, turbine or compressor cascades. Generally the flows in the previously mentioned devices are supersonic flows accompanied by condensation. The supersonic flow in turbine cascades was studied by Maiorskii (1965). The flow along a wavy wall was investigated by Hosokawa(1960), Burg(1973), and Jungbluth(1974, 1975). Zierep(1972) studied analytically the inviscid sonic flow in an infinite wavy wall, using the parabolic method as a generalized approximate method. Regarding the droplet formation and condensation, Schnerr and Dohrmann(1990) investigated transonic flow around airfoils with energy supply by homogeneous condensation. Recently, Li and Zierep(1993) simulated numerically two-dimensional steady adiabatic viscous flow and inviscid flow with energy supply by homogeneous condensation in a wavy wall channel. Also, Kwon(1994) studied the characteristics of the supersonic flow with condensation along a wavy wall in a channel.

In the present study, the characteristics of Prandtl-Meyer expansion of supersonic flow with condensation along a wavy wall in a channel are investigated for the case of moist air flow by both experiments and numerical analyses. In the experiments, the flow fields are visualized by a Schlieren system and the distributions of static pressure along the upper wavy wall are measured by a scanning valve system. As a numerical method, the two-dimensional direct marching method of characteristics is used with the assumption that the flow is inviscid. The effects of stagnation temperature, absolute humidity, and attack angle of the upper wavy wall on the generation and reflection process of the oblique shock wave are clarified.

2. Experimental Apparatus and Method

The experiments are carried out in an intermittent indraft supersonic wind tunnel with the respective capacities of $40m^3$ in the stagnation reservoir and $5m^3$ in the vacuum tank as shown in Fig. 1. The pressure in the vacuum tank are kept below 0.2kPa by a vacuum pump. When the isolation valve downstream of the test section is opened, the moist air in the reservoir expands to the vacuum tank, so that the steady state in the test section is maintained approximately for the duration of 15 seconds.

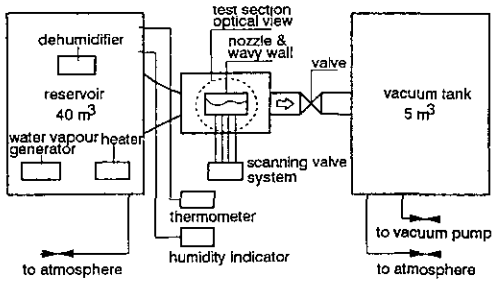

Fig. 1 Schematic diagram of experimental apparatus

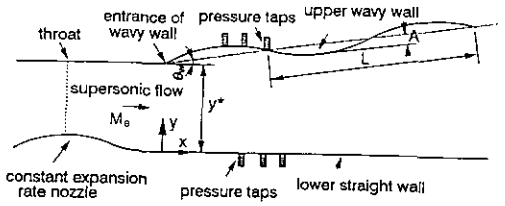

Fig. 2 Schematic of test section with a wavy wall in a channel

The schematic of the test section with the upper wavy wall and the lower straight wall is shown in Fig. 2. The height y^* and the Mach number M_e at the wavy wall entrance are 23mm and 1.4 respectively. The attack angles θ_w of the centerline of the upper wavy wall to x-axis are 4°, 7° and 10°. The amplitude A and the period L of the wavy wall are 1.5mm and 80mm respectively. The shape of the upper wavy wall is represented by

$$y(x)=y^*+\frac{A}{\cos(\theta_w)}\cdot\sin\left\{\left(\frac{2\pi x}{L}\right)\cdot\frac{1}{\cos(\theta_w)}\right\}+x\tan(\theta_w) \quad (1)$$

The channel is perforated with 25 holes along the upper wavy wall spaced at the intervals of 4 ~5mm to measure the static pressure.

In the experiment, moist air is used as working fluid. In order to study the supersonic flow with

condensation along a wavy wall in the test section, the flow should be expanded to supersonic flow without nonequilibrium condensation at the inlet of the test section. For this purpose, a supersonic half nozzle with a constant expansion rate is installed at an upstream position of the test section as shown in Fig. 2."

Moist air is expanded to 1.4 in Mach number without nonequilibrium condensation through a supersonic half nozzle with constant expansion rate. The Mach number M_e at the wavy wall entrance is confirmed by the area ratio of the wavy wall entrance to the throat and by the static pressure measured at the entrance.

In order to get the required stagnation relative humidity ϕ_0 at the reservoir, the stagnation relative humidity ϕ_0 is controlled by a dehumiditier, a water vapour generator, a heater and a circulation fan at the reservoir. In this case, the pressure p_0 at the stagnation condition is constant at 101kPa. The stagnation relative humidity ϕ_0 is measured by a digital humidity indicator (CHINO Co., model HN-K)."

The flow fields are visualized by a Schlieren system. It consists of a Xe-light source, two concave mirrors with the focal leagth of 3000mm and a visualization camera. The distributions of pressure along the upper wavy wall are measured by a scanning valve system with the pressure transducers of Druck company with the model number, PCB 112A21. The scanning valve system has 40 channels, and the time constant can be set from 0.1 to 1.0 second.

3. Numerical Procedure

In order to analyze the two-dimensional steady state supersonic flow with condensation, the direct marching method of characteristics is used as a numerical method. The governing equations are transformed to the characteristic equations through some modifications suggested by Vincenti(1965). The domain of calculation is same as that of the experimental test section in Fig. 2. In the numerical calculation, it is assumed that the flow expands isentropically from the stagnation condition to the wavy wall entrance, and that all of the flow properties at the initial calculation line of the y-direction (that is, at the wavy wall entrance) are uniform. On the other hand, since it can be supposed that streamlines near the upper wavy and the lower straight walls go along with two walls, boundary conditions for θ are as follows.

At the lower straight wall

$$\theta=0 \tag{2}$$

$$along\ y(x)=0 \tag{3}$$

At the upper wavy wall

$$\theta=\tan^{-1}\left[\frac{dy}{dx}\bigg|_{\text{wall profile}}\right]$$
$$=\tan^{-1}\left[\left\{\frac{2\pi A}{L\cos^2(\theta_w)}\right\}\cdot\cos\left\{\left(2\pi\frac{x}{L}\right)\cdot\frac{1}{\cos(\theta_w)}\right\}+\tan(\theta_w)\right] \tag{4}$$

$$along\ y(x)=y^*+\frac{A}{\cos(\theta_w)}\cdot\sin\left\{\left(\frac{2\pi x}{L}\right)\cdot\frac{1}{\cos(\theta_w)}\right\}+x\tan(\theta_w) \tag{5}$$

The very complex problem, which appears where the overlappings of crossing of the same family characteristics occur, can be solved satisfactorily by the modified method suggested by Zucrow(1977).

4. Results and Discussions

4.1 Experimental results

4.1.1 Flow pattern

Figure 3 shows the Schlieren photograph and the distribution of dimensionless static pressure along the upper wavy wall. A Prandtl-Meyer expansion wave is generated at the entrance of the wavy wall. From $x=10$mm to $x=30$mm of the upper wavy wall, compression waves are generated by the effect of the upper wavy wall geometry, run to point A, interact with the boundary layer and become oblique shock wave AB. This wave reflects again to point E and goes to point F. Especially near point A, a new oblique shock CD is generated by coalescence of compression waves which result from the separation of the boundary layer. This flow pattern is

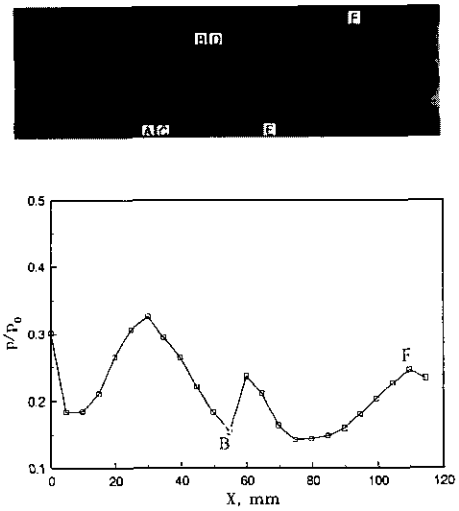

Fig. 3 Schlieren photograph and distribution of static pressure along upper wavy wall(θ_w=4°, T_0=288K, p_0=101kPa, ϕ_0=45%, M_e=1.4)

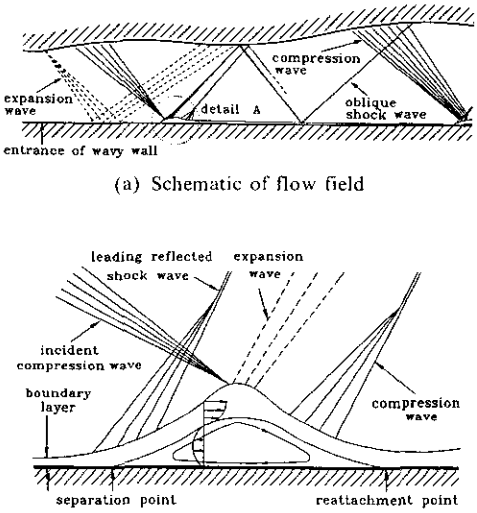

Fig. 4 Schematic of interaction between oblique shock wave and boundary layer(θ_w=4°, T_0=293K, p_0=101kPa, ϕ_0=45%)

shown schematically in Fig. 4. It shows the same flow pattern as Ikui and Matsuo(1983) suggested. The oblique shock waves AB and CD in Fig. 3 correspond to the leading reflected shock wave and the compression wave in Fig. 4, respectively. The small flaws in the Schlieren photograph of Fig. 3 are stain on the optical glass.

4.1.2 Effects of stagnation temperature, attack angle and absolute humidity

Figure 5 shows the effect of stagnation temperature T_0 on the distribution of static pressure and Mach number along the upper wavy wall. The distributions of Mach number are calculated from those of the static pressure measured along the upper wavy wall. Static pressure decreases and Mach number increases rapidly because of Prandtl-Meyer expansion caused by the positive attack angle from the wavy wall entrance to x= 10mm along the upper wavy wall and of the expansion effect caused by the area increase of flow field.

From x=10mm to x=30mm whose points coincide with the points of the first and second inflexion of the upper wavy wall, pressure increases rapidly because the effect of compression caused by the negative value of the gradient of θ(θ is the angle of inclination of the streamline with respect to the x-axis) is larger than that of the expansion caused by the area increase. From x=30mm to 56mm, pressure decreases (i.e. expansion occurs) and Mach number increases rapidly because of the expansion effect caused by expansion waves which are generated by Prandtl-Meyer expansion and are reflected from the lower wall.

On the other hand, near point A of the lower straight wall, oblique shock wave CD exists, as the compression waves that occurred from x= 10mm to 30mm along the upper wavy wall run into the lower straight wall and interact with the boundary layer. Pressure increases rapidly from x=56mm to 60mm along the upper wavy wall by the incidence of the oblique shock waves AB and CD.

From x=60mm to 74mm along the upper wavy wall, rapid expansion occurs due to the area increase. Mach number decreases from x=74mm to 110mm because of the compression effect of the upper wavy wall and oblique shock wave EF which is reflected by oblique shock wave BE. Regardless of stagnation temperature T_0, the flow patterns appear similarly. However, for the same stagnation relative humidity ϕ_0, as the stagnation temperature increases, the absolute humidity

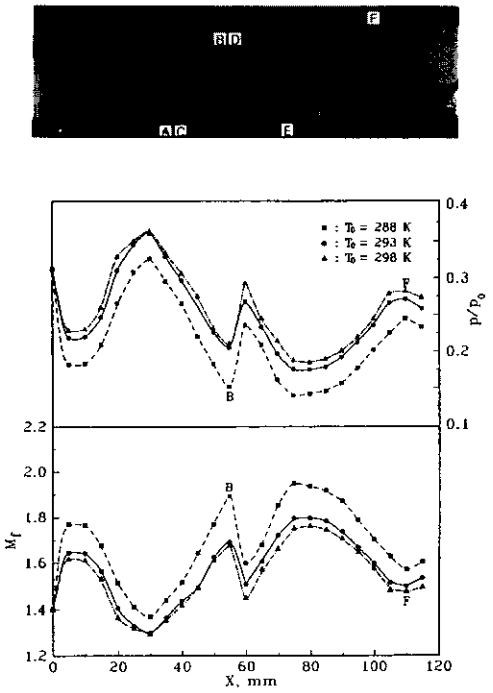

Fig. 5 Effect of stagnation temperature on distribution of static pressure and Mach number along upper wavy wall
(θ_w=4°, p_0=101kPa, ϕ_0=45%)

increases, so that the larger amount of latent heat by condensation will be released even for the case of the same Mach number at the wavy wall entrance. Therefore, as stagnation temperature for the same ϕ_0 increase, Mach number along the upper wavy wall decreases in general.

Figure 6 shows the effect of the attack angle on Mach number. For cases of the attack angles θ_w= 4° and θ_w=7°, the two flows show the similar trend. For the same inlet flow condition, increase of the attack angle shows two contradicting effects in the flow: one is acceleration effect by strengthening the Prandtl-Meyer expansion at the entrance of wavy wall, the other is deceleration effect by strengthening the adding of condensation latent heat.

For the cases of the same inlet Mach number, stagnation temperature and relative humidity, the first incident point A of the compression waves for the larger attack angle moves downstream. Also, point B which is the reflecting point of the

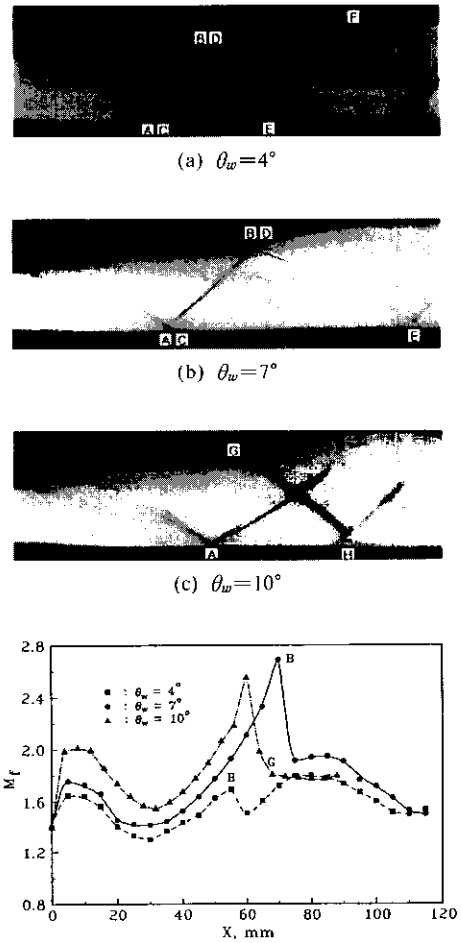

Fig. 6 Effect of attack angle on Mach number(T_0= 293K, ϕ_0=45%)

incident wave from point A, moves farther downstream in the case of θ_w=7° than θ_w=4°. From which, we can deduce that the effect of expansion becomes more dominant than that of compression due to the increase of attack angle in the present experimental condition. So in general, Mach number is higher at θ_w=7° than at θ_w=4° for the same x due to larger expansion effect. However, it turns out that the trend between θ_w=10° and θ_w=7° (or θ_w=4°) is different from that between θ_w=7° and θ_w=4°, i.e. as can be seen in the Schlieren photograph, the maximum Mach number at θ_w=10° is lower than that at θ_w=7° due to the separation near the x=70mm of the upper wavy wall. Also, a oblique shock wave GH

(a) $\omega_0=0.002(T_0=283\text{K},\ \phi_0=32\%)$

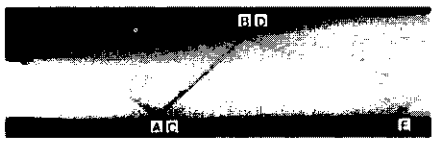

(b) $\omega_0=0.006(T_0=293\text{K},\ \phi_0=41\%)$

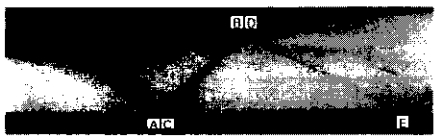

(c) $\omega_0=0.01(T_0=298\text{K},\ \phi_0=55\%)$

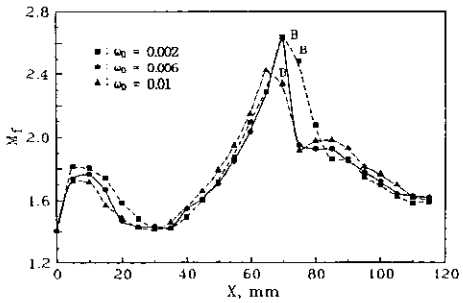

(d) Distribution of Mach number

Fig. 7 Effect of absolute humidity on Mach number ($\theta_w=7°$)

occurs newly due to the separation of boundary layer near $x=70$mm, and oblique shock wave which is reflected from point A can not penetrate into the upper wavy wall but runs into the separated boundary layer and reflects again downward.

Figure 7 shows the effect of absolute humidity ω_0 on the Mach number. For the same Mach number at the wavy wall entrance and the same attack angle, as the absolute humidity ω_0 increases, the incident points A and B move upstream. As a whole, as absolute humidity ω_0 increases, because of nonequilibrium condensation, the Mach number decreases. Especially for the case of Fig. 7(c), the boundary layer just behind

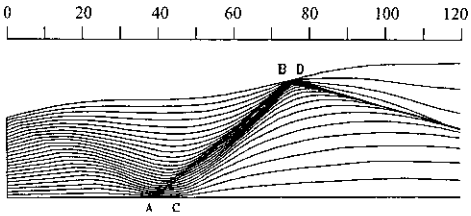

(a) Streamline

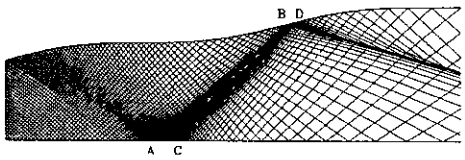

(b) Frozen Mach line

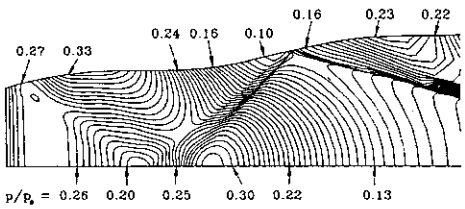

(c) Iso-pressure

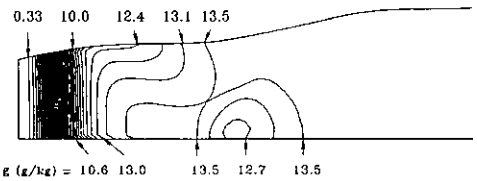

(d) Iso-mass fraction of liquid

Fig. 8 Plots of calculated results($\theta_w=7°$ $T_0=298$K, $p_0=101$kPa, $\phi_0=55\%$)

point B at the upper wavy wall is separated as a result of the interaction among the oblique shock waves AB, CD and the boundary layer. Point E, where the oblique shock wave runs into the lower wall from the upper wavy wall, moves farther upstream in the case of $\omega_0=0.01$ (Fig. 7(c)) than $\omega_0=0.006$ (Fig. 7(b)). This is owing to the increase of latent heat addition resulting from condensation as absolute humidity ω_0 increases for the same Mach number at the wavy wall entrance and geometry of the channel.

4.2 Numerical results

Figure 8 shows the results of numerical analysis. According to the streamline plot, the compression waves which are generated from $x=$ 10mm to $x=30$mm along the upper wavy wall run into the lower wall and form the oblique shock wave AB. Then they reflect again from the upper wavy wall, form the oblique shock wave downward. This result shows the same flow pattern as Fig. 7(c) with the same inlet flow condition.

As shown in the distribution of frozen Mach lines, the compression waves run into near $x=$ 46mm on the lower straight wall and are accumulated. These accumulated waves make weak oblique shock wave. Mach waves, which are generated near $x=35$mm on the upper wavy wall, run into the lower wall, form a regular reflection of compression waves and are added to the weak oblique shock wave, so that this addition of the compression waves to the oblique shock wave AB strengthens the shock strength. On the other hand, a Prandtl-Meyer expansion fan which is generated at the wavy wall entrance runs into near $x=30$mm of the lower wall and reflects regularly. According to iso-pressure distribution, dimensionless static pressure reaches the peak value of $p/p_0=0.33$ near $x=25$mm of the upper wavy wall. Shock strength is higher at point B ($\Delta p/p_1=0.59$) than at point A ($\Delta p/p_1=0.20$). According to iso-liquid mass fraction, the values of liquid mass fraction near the upper wavy wall are smaller than that near the lower wall in general for the same x. This is caused by fact that the expansion effect by angle θ_w at the upper wall i. e. the effect of area increase is larger than the compression effect due to the geometrical shape of the upper wavy wall so that local supersaturation is higher at the upper wavy wall than at the lower wall. On the other hand, point B moves farther downstream in the numerical analysis than in the experiment. This is the reason that the fluid is assumed to be inviscid in numerical analysis.

Figure 9 shows the locations of incident points (typically, points A and E shown in Fig. 3) of compression waves and oblique shock waves with the variations of stagnation absolute humidity ω_0 and attack angle θ_w. For the same attack angle, as absolute humidity ω_0 which will be related directly to the amount of heat addition to the surrounding supersonic flow by nonequilibrium condensation increases, incident points A of the compression waves and E of the oblique shock wave move slightly upstream. For the case of the same ω_0, the incident points A and E move downstream as the attack angle θ_w increases because of the expansion effect resulting from the increase of attack angle. On the other hand, it is observed from the Schlieren photograph that con-ensation shock waves are generated for the case of $\omega_0>0.0075$. In this figure, CSW stands for condensation shock wave.

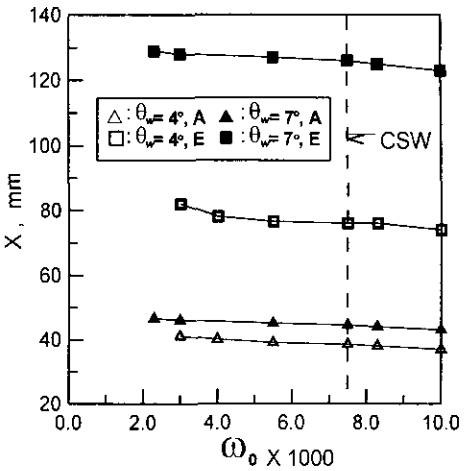

Fig. 9 Incident points of compression wave and oblique shock wave with variations of absolute humidity and attack angle

5. Conclusions

As the results of experimental and numerical study on Prandtl-Meyer expansion of supersonic flow with condensation along a wavy in a channel, the following conclusions are obtained.

(1) For the cases of the same inlet Mach number and stagnation relative humidity, the distribution of Mach number generally decreases because of latent heat addition resulting from condensation, as the stagnation temperature increases.

(2) For the cases of the same inlet Mach number and relative humidity, the first incident point

A of the compression waves for a larger attack angle moves downstream, because the expansion effect by an increased attack angle is larger than the compression effect by condensation. Also, the reflection point B moves further downstream in the case of $\theta_w=7°$, as compared with the case of $\theta_w=4°$.

(3) For the cases of the same inlet Mach number and attack angle, the incident point A and the reflection point B move upstream, as the stagnation relative humidity increases.

(4) The wavy wall plays an important role in the generation of an oblique shock wave.

(5) It turns out that the results of the numerical analysis agree well with those of the experiments.

References

Burg, K., Viriyabhun, S. and Zierep, J., 1973, "The Supersonic Flow Along a Wavy Wall with Straight Wall" *Acta Mechanica*, Vol. 16, p. 271.

Frank, W., 1985, "Condensation Phenomena in Supersonic Nozzles," *Acta Mechanica*, Vol. 54, pp. 135~159.

Hosokawa, I., 1960, "Transonic Flow Past a Wavy Wall," *J. Phys. Soc. Japan*, Vol. 15, pp. 2080~2086.

Ikui, T. and Matsuo, K., 1983, *Mechanics of Shock Waves*, Corona Pub., pp. 108~109.

Jungbluth, H., 1974, *Fluid Mechanics and Fluid Machine*, Verlag G. Braun. Karlsruhe, p. 41.

Jungbluth, H., 1975, "Experiment for Subsonic Flow Along a Wavy wall," *Acta Mechanica*. Vol. 22, pp. 171~180.

Kwon, S. B., Kim, B.J., Ahn H.J. and Jeon, H. K., 1994, "The Study of Supersonic Flow with Condensation along a Wavy Wall in a Channel," *Trans. KSME*, Vol. 18, No. 2, pp. 424~431 in Korea.

Li, P. and Zierep, J., 1993, "Periodic Transonic Flow Without and With Condensation in a 2-D Plane Channel," *Acta Mechanica*, Vol. 100, pp. 1~12.

Maiorskii, E.V. and Troyanovskii, B.M., 1965, "An Experimental Study of Supersonic Flow in Turbine Cascade," *Teploenergetika*, Vol. 12, pp. 69~72.

Schnerr, G.H., and Dohrmann, U., 1989 and 1990, "Transonic Flow Around Airfoils with Relaxation and Energy Supply by Homogeneous Condensation," *AIAA Paper*, Vol. 89, No. 1834, and *AIAA J.* Vol. 28, pp. 1187~1193.

Zierep, J., 1972, "The Transonic Round Flow Along Wavy Wall with Shock wave," *Roumanian J. Tech. Sci. Appl. Mech.*, Vol. 17, pp. 721~729.

Zucrow, M.J. and Hoffman, J.D., 1977, *Gas Dynamics*, John Wiley & Sons, Inc., p. 143.